HHS Public Access

Author manuscript

J Inorg Biochem. Author manuscript; available in PMC 2017 November 01.

Published in final edited form as:

J Inorg Biochem. 2016 November ; 164: 1–4. doi:10.1016/j.jinorgbio.2016.06.028.

Organometallic myoglobins: Formation of Fe–carbon bonds and distal pocket effects on aryl ligand conformations

Bing Wang, **Leonard M. Thomas**, and **George B. Richter-Addo**

Department of Chemistry and Biochemistry, and Price Family Foundation Institute of Structural Biology, University of Oklahoma, Norman 73019, United States. FAX: 405-325-6111. Tel: 405-325-6401

Abstract

Bioorganometallic Fe–C bonds are biologically relevant species that may result from the metabolism of natural or synthetic hydrazines. The molecular structures of four new sperm whale mutant myoglobin derivatives with Fe–aryl moieties, namely H64A–tolyl-*m*, H64A–chlorophenyl-*p*, H64Q–tolyl-*m*, and H64Q–chlorophenyl-*p*, have been determined at 1.7-1.9 Å resolution. The structures reveal conformational preferences for the substituted aryls resulting from attachment of the aryl ligands to Fe at the site of net $-NHNH_2$ release from the precursor hydrazines, and show distal pocket changes that readily accommodate these bulky ligands.

Keywords

iron-carbon; arylhydrazine; crystal structure; heme; myoglobin

Arylhydrazines ($ArNHNH_2$; Ar = aryl) occur in nature and are important chemical species in both agrochemical and pharmaceutical industry [1]. Synthetic hydrazines are also prevalent in the general environment [2]. In some cases, hydrazines are beneficial components of pharmaceutical drugs such as the antidepressant drugs isoniazid and phenelzine, but are also toxic and can act as cancer causative agents [1, 2]. For example, the newly FDA-approved drug DUOPA® for Parkinson's disease contains the substituted hydrazine carbidopa with a known hemolytic anemia side effect. The parent hydrazine (NH_2NH_2) is found in tobacco and tobacco smoke [3]. Hydrazines can also be present in certain foods. For example, 4-hydroxymethylphenylhydrazine is generated as a metabolite from agaritine, a food component from the edible commercial mushroom *Agaris bisporus* [4].

Phenylhydrazine is toxic to red blood cells [5], and the hemoglobin-phenylhydrazine reaction has been used to model hemolytic anemia. Interactions of substituted hydrazines

Correspondence to: George B. Richter-Addo.

Supporting Information: Experimental procedures and UV-vis spectra (Figures S1-S3); Table of X-ray data collection and refinement statistics (Table S1); additional X-ray structure figures (Figures S4-S5).

with human hemoglobin (Hb) may also result in hemolysis, Heinz-body formation, and degradation of the protein [6]. Related interactions of substituted hydrazines and diazenes (RN=NH) with other heme proteins such as myoglobin (Mb) [7-9], cytochrome P450 [10-12], and catalase [13] have been reported [14]. The generated products often contain heme σ-aryl bonds with direct Fe–C(aryl) linkages (Scheme 1) as determined by UV-vis and NMR spectroscopy. In some cases, an Fe–to–N(porphyrin) migration of the aryl ligand (Scheme 1; right) occurs upon extraction of the heme from the protein, or occurs within the heme protein active site (for cytochrome P450) [14].

Only two X-ray crystal structures have been reported to date for such heme protein σ-aryl species. The preparation and crystal structure of the prototypical wild-type (wt) sperm whale (sw) Mb–phenyl complex, obtained from the reaction of ferric Mb (metMb) with phenylhydrazine, was published by Ringe and Ortiz de Montellano and coworkers in 1984 [7]. The related preparation and crystal structure of the cytochrome $P450_{cam}$–phenyl complex, obtained from the reaction with phenyldiazene, was reported by Poulos and Ortiz de Montellano and coworkers in 1990 [12].

The potential of arylhydrazines to serve as steric probes for heme protein active sites has been evaluated [14]. It is well established that the arylhydrazine reactions with heme proteins proceed via carbon-based radicals [15, 16] formed during aerobic reaction with the protein en route to Fe–C bond formation [17]. New X-ray structural data that clarify which aryl C atoms bind to the Fe centers, and information regarding preferred aryl ligand orientations from reactions involving substituted arylhydrazines as a function of active site structure are thus desirable.

We have prepared a representative set of derivatives from the reactions of arylhydrazines with wt and mutant Mbs (Chart 1) to determine the mode of attachment of the substituted aryl groups to the iron centers [18], and the effect of mutating the distal pocket H64 residue on the orientation of the aryl ligands. We chose the H64A mutant to remove distal sidechain H-bonding, and the H64Q mutant to provide an alternate H-bonding capacity in the heme pocket.

The aerobic reaction of sw metMb with phenylhydrazine results in spectral changes in the UV-vis spectrum identical to those reported previously (Supporting Information Figure S1) [8, 9]. The related reaction of the metMb H64A mutant (λ_{max} 408 nm) [19] with *m*-tolylhydrazine in phosphate buffer at pH 7.4 reveal similar spectral features to generate a product (λ_{max} 436 nm), shown in Figure 1A. When *p*-chlorophenylhydrazine is used for the reaction, similar spectral shifts are observed (Figure 1B). Both reactions are essentially complete after ~1.5 min (Figure S2 in the SI). Reactions of the metMb H64Q mutant [19] with *m*-tolylhydrazine and *p*-chlorophenylhydrazine proceed similarly, with the reactions being complete after ~6 min and ~3 min, respectively (Figure S3 in the SI).

We have successfully obtained the X-ray crystal structures of all four myoglobin H64A–tolyl-*m* (1.77 Å resoln), H64A–chlorophenyl-*p* (1.70 Å resoln), H64Q–tolyl-*m* (1.88 Å resoln), and H64Q–chlorophenyl-*p* (1.87 Å resoln) derivatives. We also reproduced the crystal structure of the known wt sw Mb–phenyl complex [7] at 1.87 Å resolution (Figure S4

in the SI). Careful exposure of the respective pre-formed metMb crystals to solutions of the arylhydrazines in air resulted in the formation of products that retained their crystallinity.[1] Numerous trials (>40 trials for each derivative) were needed to obtain suitable product crystals with good diffraction, as this reaction generally resulted in disruption of crystallinity and crystal cracking. Indeed, we have not yet obtained suitable crystals for the wt Mb derivatives with the tolyl and chlorophenyl ligands.

The heme sites of the Mb H64A and H64Q products are shown in Figure 2, and demonstrate direct Fe–C bond formation to generate the product complexes. The Fe–C bond lengths of 1.9–2.0 Å are similar to those obtained in heme model Fe–aryl compounds (~1.96 Å) [20].

The tolyl ligand in the H64A–tolyl-*m* derivative (Figure 2A) is bound to Fe via the carbon atom bearing the initial hydrazine functional group (i.e., in the *meta* position). The aryl methyl substituent points to the hydrophobic interior of the protein, with the closest contact of 3.4 Å between the ligand methyl C-atom and the δ_2 C-atom of Leu29. The aryl plane essentially eclipses diagonal porphyrin N atoms, and is perpendicular to the heme N_4-plane (with a small ~5° tilt to the heme normal).

In the H64A–chlorophenyl-*p* structure (Figure 2B), the aryl ligand binds via *the para-C* atom which held the hydrazine moiety. The ligand plane also eclipses diagonal porphyrin N-atoms, but has a larger (~18°) tilt from the normal to the heme plane in the direction of Phe43 and Phe46, with the closest calculated distance being between the centroid of the aryl ring and $C\gamma_2$ of Val68.

The structures of the H64Q derivatives are similar to those of the H64A mutant in terms of the points of attachment of the aryl ligands to the Fe centers and these ligands eclipsing diagonal porphyrin N atoms. However, although the tolyl ligand plane (Figure 2C) has a similar tilt (~8°) with respect to the heme normal as seen in the H64A derivative, the chlorophenyl ligand plane (Figure 2D) has a significantly smaller (~7°) tilt from the heme normal than that observed in the H64A mutant (~18°). The calculated distances between the chlorophenyl ligand atoms (Figure 2D) and closest distal pocket residues are >3.6 Å.

The X-ray crystal structures in Figure 2 provide valuable information that can be used to address substituent and distal pocket influences on the ligand conformation in these bioorganometallic Fe–C complexes. A superposition of these structures on those of the respective sw metMb precursors [21][19][22] is shown in Figure 3. As noted above, both the H64A and H64Q mutants gave the same reaction products upon reactions with the arylhydrazines, both in terms of ligand identity and mode of attachment, with no clear

[1]To obtain the crystal structure of the Mb-aryl products, crystals of the respective metMb precursor [19] were placed in a droplet (4 μL) on a cover slide that contained a solution of the arylhydrazine (0.0125 M arylhydrazine dissolved in 100 mM Tris•HCl, 1 mM EDTA, pH 7.4 or 9.0, and 3.0 M ammonium sulfate). The cover slide was flipped over and placed on top of a well (in a 24-well format) and sealed with grease; the well contained 100 mM Tris•HCl, 1 mM EDTA, pH 7.4 or 9.0, and 3.0 M ammonium sulfate. This allowed the metMb crystals in the drop to react with the arylhydrazines for 1-14 days at room temperature without drying out. During this process, the cover slides were opened every 2-3 days, and the reaction solutions were exchanged with fresh aerated arylhydrazine solutions (and fresh air introduced into the well volume) in order to ensure completion of the reactions. The product crystals were harvested by cryoloops and washed with cryosolution (100 mM Tris•HCl, 1 mM EDTA, pH 7.4 or 9.0, 3 M ammonium sulfate, 10% glycerol) and stored in liquid nitrogen. The structures reported here were obtained using the following conditions: (i) H64A at pH 9; ligand soaking times of 2 days for the *m*-tolyl derivative and 14 days for the *p*-chlorophenyl derivative, (ii) H64Q at pH 7.4; ligand soakings of 2 days for the *m*-tolyl derivative and 3 days for the *p*-chlorophenyl derivative.

hydrogen-bonding interactions involving the ligands. We focus our discussion on the sidechains of the residues Val68, Gln64, and Phe46, and the CD loop region.

In the H64A–tolyl-*m* structure, the Val68 sidechain flips to a “vertical” orientation from its initial horizontal orientation in the metMb H64A structure, creating a 3.7 Å distance between this sidechain and the centroid of the aryl ring. This Val68 flip relieves a steric clash with the tolyl ligand. In contrast, the Val68 sidechain does not flip in the H64A–chlorophenyl structure, probably due to the significant ~18° tilt of the aryl ligand from the heme normal and away from this residue. Interestingly, this same aryl ligand tilt results in a 45° rotation of the aryl plane of Phe46 and its subsequent movement away from the heme pocket. Within the backbone structure, the largest change occurs in the H64A–chlorophenyl derivative when compared with the metMb precursor and the tolyl complex. In the H64A–chlorophenyl derivative, a ~1.0 Å downward movement of the CD loop region that contains Phe46 is evident (Figure S5 in the SI), and is likely associated with the change in Phe46 orientation induced by the chlorophenyl tilt in the pocket.

In the related H64Q derivatives, the Val68 sidechains flip to a vertical orientation for both the tolyl and chlorophenyl complexes, when compared with the starting H64Q metMb structure (Figure 3B). Interestingly, a major orientation change occurs for the Gln64 sidechains in the tolyl and chlorophenyl derivatives from the original position in the H64Q metMb precursor where it H-bonds with the H_2O ligand to Fe. The new Gln64 orientation in the tolyl and chlorophenyl derivatives establishes a new H-bonding contact with Asp60 thus stabilizing this conformation. To the best of our knowledge, this Gln64 orientation shift away from the distal pocket interior towards the exterior is the first such observed movement in any single or multi-mutant H64Q structure reported. Unlike that observed in the H64A structures, no significant movement of the CD loop region is observed in these H64Q structures.

There are several other points to note regarding the crystal structures shown in Figures 2 and 3. First, these products resulting from a rather complicated reaction of arylhydrazines with the metMb heme proteins were obtained from soaking pre-formed crystals of the metMb precursors with the arylhydrazine reagents, and show only one preferred conformation for each of the bound aryl ligands. Given that both H64A and H64Q mutants gave the same ligand identities in the products, it seems that the nature of the distal pocket mutation is relatively unimportant in these reactions reported here. The results also suggest that the aryl radical intermediates that form during the heme-induced reaction are generated in close proximity to the Fe centers to enable rapid attachment of the ligands to the Fe, resulting in a single attachment isomer from the arylhydrazine precursors. Consistent with previous NMR studies by others on wt sw Mb–aryls [9, 17], we do not observe any migrations of the aryl ligands to heme pyrrole N-atoms. The observed distal pocket changes suggest a role for Val68 in that it may flip its orientation as a function of bound ligand to accommodate varied sizes and/or orientations of the ligands. Further, larger aryl ligands can be accommodated with additional changes in other distal pocket residues such as Phe46 with concomitant movements in the CD loop region. Notably, the distal pocket Gln sidechains in the H64Q mutant products display significant movement towards the protein exterior to accommodate the new ligands.

Given the known interactions between hydrazine derivatives and hemoglobins, and their associated relationships to hemolysis and other deleterious effects, the new structures obtained from this work provide an expanded framework for an improved understanding and interpretation of structure-function studies in this important area.

Supplementary Material

Refer to Web version on PubMed Central for supplementary material.

Acknowledgments

G.B.R.-A. thanks the National Science Foundation (CHE-1213674) for financial support for this work. X-ray data reported in this publication were in part collected in the OU Macromolecular Crystallography Laboratory (MCL), which is supported, in part, by an Institutional Development Award (IDeA) from the National Institute of General Medical Sciences of the National Institutes of Health under grant number P20GM103640.

References

1. Malcamor L, Stark AA. Mutagenicity and toxicity of carcinogenic and other hydrazine derivatives - correlation between toxic potency in animals and toxic potency in *Salmonella-typhimurium* Ta1538. Appl Environ Microbiol. 1982; 44:801–808. [PubMed: 6756304]
2. Toth B. Synthetic and naturally occurring hydrazines as possible cancer causative agents. Cancer Res. 1975; 35:3693–3697. [PubMed: 1238167]
3. Liu YY, Hoffmann D. Quantitative chromatographic determination of maleic hydrazide in cigarette smoke. Anal Chem. 1973; 45:2270–2273.
4. Sinha BK, Mason RP. Biotransformation of hydrazine derivatives in the mechanism of toxicity. J Drug Metab Toxicol. 2014; 5:1000168.
5. Berger J. Phenylhydrazine haematotoxicity. J Appl Biomed. 2007; 5:125–130.
6. Beaven GH, White JC. Oxidation of phenylhydrazines in the presence of oxyhaemoglobin and the origin of heinz bodies in erythrocytes. Nature. 1954; 173:389–391. [PubMed: 13144768]
7. Ringe D, Petsko GA, Kerr DE, Ortiz de Montellano PR. Reaction of myoglobin with phenylhydrazine: A molecular doorstop. Biochemistry. 1984; 23:2–4. [PubMed: 6691963]
8. Swanson BA, Ortiz de Montellano PR. Structure and absolute stereochemistry of the 4 *N*-phenylprotoporphyrin-IX regioisomers isolated from phenylhydrazine-treated myoglobin. J Am Chem Soc. 1991; 113:8146–8153.
9. Ortiz de Montellano PR, Kerr DE. Inactivation of myoglobin by ortho-substituted arylhydrazines. Formation of prosthetic heme aryl-iron but not *N-aryl* adducts. Biochemistry. 1985; 24:1147–1152. [PubMed: 4096894]
10. Battioni P, Mahy JP, Delaforge M, Mansuy D. Reaction of monosubstituted hydrazines and diazenes with rat-liver cytochrome-P450: Formation of ferrous-diazene and ferric σ-alkyl complexes. Eur J Biochem. 1983; 134:241–248. [PubMed: 6873062]
11. Muakkassah SF, Yang WCT. Mechanism of the inhibitory-action of phenelzine on microsomal drug metabolism. J Pharmacol Exp Ther. 1981; 219:147–155. [PubMed: 7288604]
12. Raag R, Swanson BA, Poulos TL, Ortiz de Montellano PR. Formation, crystal-structure, and rearrangement of a cytochrome P450cam iron phenyl complex. Biochemistry. 1990; 29:8119–8126. [PubMed: 2261467]
13. Ortiz de Montellano PR, Kerr DE. Inactivation of catalase by phenylhydrazine: Formation of a stable aryl-iron heme complex. J Biol Chem. 1983; 258:10558–10563. [PubMed: 6885792]
14. Ortiz de Montellano PR. Arylhydrazines as probes of hemoprotein structure and function. Biochimie. 1995; 77:581–593. [PubMed: 8589069]
15. Hill HAO, Thornalley PJ. Phenyl radical production during the oxidation of phenylhydrazine and in phenylphydrazine-induced hemolysis. FEBS Lett. 1981; 125:235–238. [PubMed: 6262132]

16. Ortiz de Montellano PR, Augusto O, Viola F, Kunze KL. Carbon radicals in the metabolism of alkyl hydrazines. J Biol Chem. 1983; 258:8623–8629. [PubMed: 6305994]

17. Kunze KL, Ortiz de Montellano PR. Formation of a σ-bonded aryliron complex in the reaction of arylhydrazines with hemoglobin and myoglobin. J Am Chem Soc. 1983; 105:1380–1381.

18. Augusto O, Kunze KL, Ortiz de Montellano PR. *N*-Phenylprotoporphyrin-IX formation in the hemoglobin-phenylhydrazine reaction: Evidence for a protein-stabilized iron-phenyl intermediate. J Biol Chem. 1982; 257:6231–6241. [PubMed: 7076671]

19. Quillin ML, Arduini RM, Olson JS, Philips GN Jr. High-resolution crystal structures of distal histidine mutants of sperm whale myoglobin. J Mol Biol. 1993; 234:140–155. [PubMed: 8230194]

20. Bill E, Schunemann V, Trautwein AX, Weiss R, Fischer J, Tabard A, Guilard R. Mossbauer investigations of the hexachlorantimonate salt of the phenyliron 2,3,7,8,12,13,17,18-octaethyl-5,10,15,20-tetraphenylporphyrinate, [Fe(oetpp)Ph]$SbCl_6$ and X-ray structure of the phenyliron(III) precursor Fe(III)(oetpp)Ph. Inorg Chim Acta. 2002; 339:420–426.

21. The crystal structures of wt sw metMb [19], H64A sw metMb [22], and H64Q sw metMb [19] have been reported.

22. Smith, RD. Ph D Thesis. Rice University; Houson, TX: 1999. Correlations between bound *n*-alkyl isocyanide orientations and pathways for ligand binding in recombinant myoglobins.

Highlights

1. Crystal structures of Fe–C(aryl) derivatives of myoglobin mutants were determined.
2. The structures reveal that the C-atom bound to the hydrazine coordinates with Fe.
3. Only one conformation of the Fe-aryl moiety was observed in each structure.

Synopsis

Bioorganometallic Fe-aryl derivatives of myoglobin mutants (H64A and H64Q) have been prepared from their myoglobin $Fe^{III}(H_2O)$ precursors and arylhydrazines. Their X-ray crystal structures reveal that the C-atom bound to the hydrazine is what attaches to Fe, and that the aryl ligands are accommodated by conformational changes in the distal pockets.

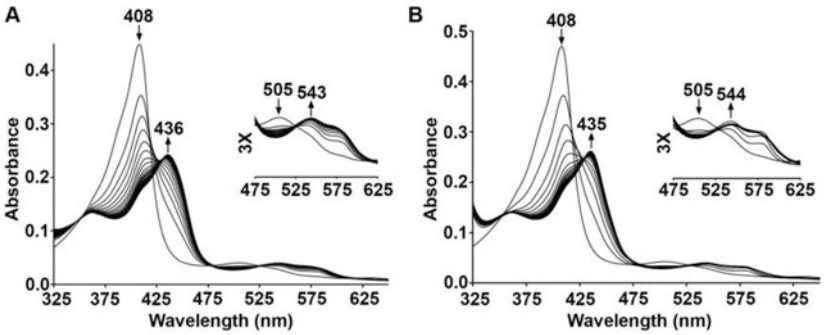

Figure 1.

UV-vis spectral changes during the reactions of H64A sw metMb with the arylhydrazine reagent (A) *m*-tolylhydrazine, and (B) *p*-chlorophenylhydrazine. Conditions: 0.1 M phosphate buffer, pH 7.4, [protein] = 2 μM, final [reagent] = 1 mM.

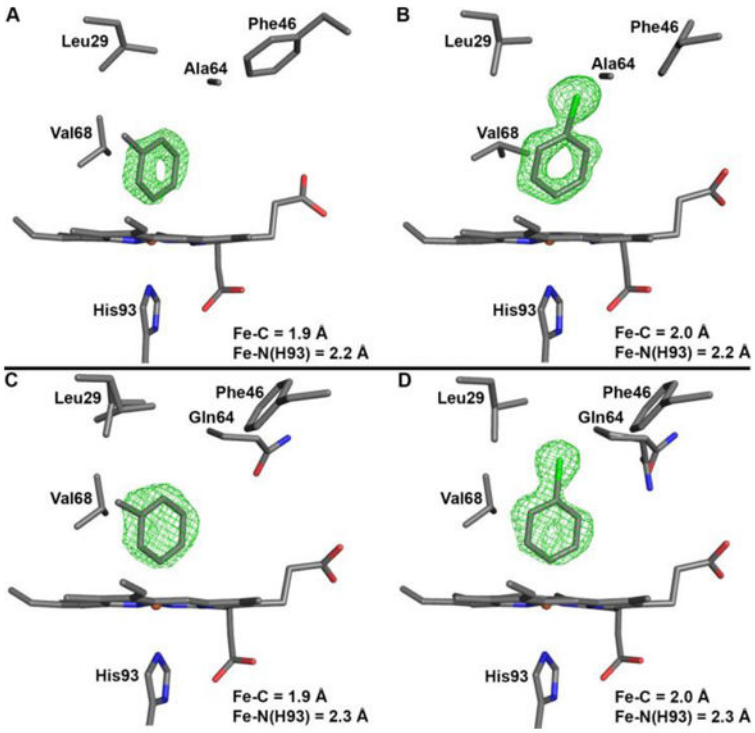

Figure 2.

Active site structures of the mutant sw Mb–tolyl and –chlorophenyl derivatives, showing the F_o–F_c omit electron density maps (in green mesh) and the final models. (A) H64A–tolyl-*m*, contoured at 2.5σ (PDB accession code 5ILE), (B) H64A–chlorophenyl-*p*, contoured at 2.5σ (PDB accession code 5ILM), (C) H64Q–tolyl-*m*, contoured at 3σ (PDB accession code 5ILP), (D) H64Q–chlorophenyl-*p*, contoured at 3σ (PDB accession code 5ILR).

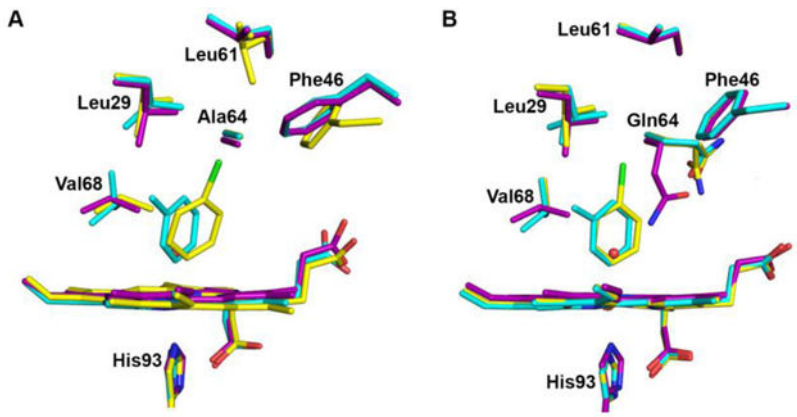

Figure 3.

Heme site comparisons between the mutant metMb and product complexes. A) metMb H64A–H_2O (purple), H64A–tolyl-*m* (cyan) and H64A–chlorophenyl-*p* (yellow). B) metMb H64Q–H_2O (purple), H64Q–tolyl-*m* (cyan) and H64Q–chlorophenyl-*p* (yellow). The relative heme and amino acid residue positions were determined from Cα chain superpositions.

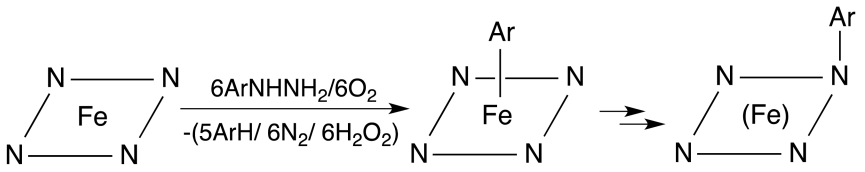

Scheme 1.

Formation of σ-aryl (middle) and *N*-aryl (right) products from the reaction of arylhydrazines with heme proteins. The heme is designated by the N_4Fe plane.

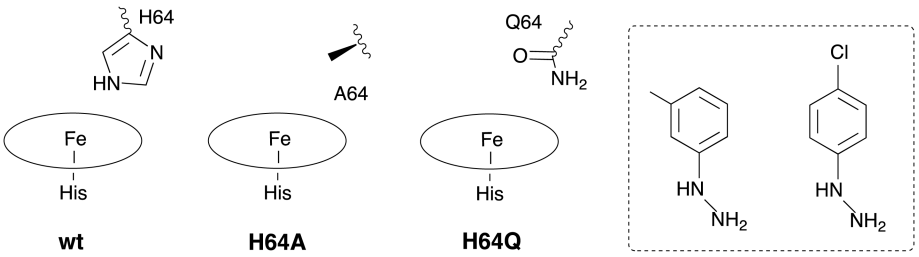

Chart 1.
Sketches of the wt and mutant Mbs, with the arylhydrazine reagents shown in the boxed area.